The Post-Illumination Pupil Response (PIPR).

Prakash Adhikari, B Optom,[1] *Andrew J. Zele, PhD,**[1] *Beatrix Feigl, MD, PhD**[1,2]

[1] Medical Retina and Visual Science Laboratories, Institute of Health and Biomedical Innovation, Queensland University of Technology, 60 Musk Avenue, Brisbane QLD 4059, Australia.

[2] Queensland Eye Institute, South Brisbane QLD, Australia.

*Corresponding Authors:

Beatrix Feigl, MD, PhD. Email: b.feigl@qut.edu.au

Andrew J. Zele, PhD. Email: andrew.zele@qut.edu.au

Abstract

Purpose: The post-illumination pupil response (PIPR) has been quantified using four metrics, but the spectral sensitivity of only one is known; here we determine the other three. To optimize the human PIPR measurement, we determine the protocol producing the largest PIPR, the duration of the PIPR, and the metric(s) with the lowest coefficient of variation.

Methods: The consensual pupil light reflex (PLR) was measured with a Maxwellian view pupillometer. Experiment 1: Spectral sensitivity of four PIPR metrics [plateau, 6 s, area under curve (AUC) early and late recovery] was determined from a criterion PIPR to a 1s pulse and fitted with Vitamin A1 nomogram (λ_{max} = 482nm). Experiment 2: The PLR was measured as a function of three stimulus durations (1s, 10s, 30s), five irradiances spanning low to high melanopsin excitation levels (retinal irradiance: 9.8 to 14.8 log quanta.cm^{-2}.s^{-1}), and two wavelengths, one with high (465nm) and one with low (637nm) melanopsin excitation. Intra and inter-individual coefficients of variation (CV) were calculated.

Results: The melanopsin (opn4) photopigment nomogram adequately describes the spectral sensitivity of all four PIPR metrics. The PIPR amplitude was largest with 1s short wavelength pulses (≥ 12.8 log quanta.cm^{-2}.s^{-1}). The plateau and 6s PIPR showed the least intra and inter-individual CV (≤ 0.2). The maximum duration of the sustained PIPR was 83.0±48.0s (mean±SD) for 1s pulses and 180.1±106.2s for 30s pulses (465nm; 14.8 log quanta.cm^{-2}.s^{-1}).

Conclusions: All current PIPR metrics provide a direct measure of the intrinsic melanopsin photoresponse. To measure progressive changes in melanopsin function in disease, we recommend that the PIPR be measured using short duration pulses (e.g., ≤ 1s) with high melanopsin excitation and analyzed with plateau and/or 6s metrics. Our PIPR duration data provide a baseline for the selection of inter-stimulus intervals between consecutive pupil testing sequences.

Keywords: intrinsically photosensitive Retinal Ganglion Cells (ipRGCs), melanopsin, pupil light reflex, post-illumination pupil response

INTRODUCTION

The pupil light reflex (PLR) is a fundamental diagnostic tool for objective and non-invasive measurement of retinal and optic nerve function in neuroophthalmic disorders.[1] The pupil control pathway receives retinal input from intrinsically photosensitive Retinal Ganglion Cells (ipRGCs) which also project to the suprachiasmatic nucleus (SCN) for photoentrainment,[2-7] and there is circadian modulation of the post-illumination pupil response (PIPR).[8, 9] Given that outer retinal extrinsic rod, cone and inner retinal intrinsic melanopsin photoresponses influence the human PLR,[2, 3, 8, 10-16] there has been interest in developing PLR protocols that quantify outer and inner retinal input.[14, 15, 17-25] An established marker of direct, intrinsic melanopsin activity is the PIPR, the sustained pupilloconstriction after light offset.[11, 26] Given ipRGCs are affected in optic nerve and retinal disease such as glaucoma,[21, 24, 27] retinitis pigmentosa,[14, 17, 20] diabetes,[22] age-related macular degeneration,[28] Leber's congenital amaurosis,[17] as well as in circadian disorders,[10] the PLR techniques may complement other clinical measures of retinal function in the healthy and diseased eye such as the electroretinography (ERG) and perimetry. Depending on the measurement paradigms, ERGs measure the summed and local photoreceptor, bipolar, and ganglion cell responses. Visual field testing with Standard Automated Perimetry (SAP) and other modes including Frequency Doubling Technology (FDT), Short Wavelength Automated Perimetry (SWAP), and flicker perimetry measure the integrity of visual pathways. In contrast, the PLR can be used to simultaneously differentiate inner retinal function (mediated via ipRGCs) and outer retinal function (mediated via rods and cones) to provide a clinical tool for diagnosis and monitoring progression of ocular disorders, with the PIPR being a specific measure of ipRGCs. The PIPR

has been reported in response to a range of stimulus durations, irradiances and wavelengths[8, 12, 14, 18, 21-24, 29] and quantified using five metrics, namely the plateau PIPR,[12, 14] redilation velocity,[8, 21] 6 s PIPR,[17] area under curve (AUC) early and late recovery[18] (metrics are defined in methods).

There are outstanding questions before the PIPR can be translated to clinical practice. First, the plateau PIPR metric in response to 10 s light pulses is the only metric shown to match the spectral sensitivity of opn4 melanopsin photopigment;[12, 14, 28] there are no reported measurements of the PIPR spectral sensitivity for the other metrics. Second, there has been no direct comparison of these different stimuli and metrics under the same conditions, and hence no consensus on which metric(s) should be used to quantify the PIPR for clinical application. For application in a clinical setting, the intra and inter-individual variability of the metrics for the different stimulus conditions must be determined in a single cohort to determine the optimum test conditions.

This study addresses these two questions. First, we determine the spectral sensitivity of the PIPR for each of the metrics. Second, we present measurements of the human PLR as a function of stimulus duration (1 s, 10 s, and 30 s), wavelength (465, 637 nm) and irradiance (9.8 to 14.8 log quanta.cm^{-2}.s^{-1}) to define the stimulus parameters which produce the largest melanopsin response and the PIPR metrics with the lowest intra and inter-individual coefficient of variation in the same cohort. Given that *in vitro* recordings in rat ipRGCs show up to a 10 hour response to continuous (480 nm) light stimulation at 12.8 log quanta.cm^{-2}.s^{-1},[26] and the PIPR has been only measured up to 60 s in humans,[12, 14] we measured the duration of the PIPR and demonstrate that the return to baseline pupil diameter after melanopsin excitation can be as long as 3 minutes post-illumination.

METHODS

Participants

A total of seven healthy participants with no ocular pathology were enrolled. None of the participants was taking any prescription medication. All participants had a visual acuity (≥ 6/6), normal contrast sensitivity (Pelli-Robson Chart), normal color vision (Lanthony Desaturated D-15 Test), an intraocular pressure of < 21 mmHg (iCare tonometer, Finland), a normal central visual field (Nidek MP-1 Microperimeter, Italy), and normal retinal nerve fiber layer thickness (Nidek RS-3000 OCT RetinaScan Advance, Japan). Anterior and posterior eye examination using slit lamp biomicroscopy revealed no pathology. The PIPR spectral sensitivity is reported for two participants (32 year old female; 31 year old male). The PLR and PIPR measurements are reported for five participants (4 male, 1 female; mean age = 32.6 ± 5.4 years SD; range = 29 to 42 years). The research followed the tenets of the Declaration of Helsinki and informed consent was obtained from the participants after explanation of the nature of the study. All experiments were conducted in accordance with Queensland University of Technology Human Research Ethics Approval (080000546). Participants were tested between 10 AM and 5 PM to minimize circadian variation on ipRGC contribution to the PIPR.[8, 9] Each participant was tested for up to 1.5 hours per day to minimize fatigue and each participated for ~30 hours in total.

Pupillometer

The PLR was measured using a custom built, extended Maxwellian view pupillometer.[23, 28, 30] The calibrated optical system comprised narrowband LED light sources (see Pupillometry Protocol for stimulus wavelengths) imaged in the pupil plane of the right eye via two Fresnel lenses (100 mm diameter, 127 mm and 70 mm focal lengths; Edmund Optics, Singapore) and a 5˚ light shaping diffuser (Physical Optics Corp., California, USA) to provide a 35.6˚ diameter light stimulus (retinal image diameter: 15.4 mm). The consensual image of the left

eye was recorded under infrared LED illumination (λ_{max} = 851 nm) with a Pixelink camera (IEEE^{-1}394, PL-B741 Fire Wire; 640 x 480 pixels; 60 frames/s) through a telecentric lens (Computar 2/3″ 55 mm and 2 X extender C-Mount). The stimulus presentation, pupil recording, and analysis were controlled by custom Matlab software (version 7.12.0, Mathworks, Massachusetts, USA). The blink artefacts were identified and extracted by a customized algorithm during software analysis of pupil recordings using linear interpolation. The spectral outputs of the LED stimuli were measured with a Spectroradiometer (StellarNet, Florida, USA) and light output was calibrated with an ILT1700 Research Radiometer (International Light Technologies, Massachusetts, USA). Details of the recording procedure can be found elsewhere.[8]

Pupillometry Protocol

Spectral sensitivity of the PIPR was measured with the Maxwellian view optical system in response to a 1 s rectangular pulse at five wavelengths (409 nm, 464 nm, 508 nm, 531 nm, and 592 nm). The participant's left eye was dilated (1% Tropicamide) and the criterion consensual PIPR of the fellow eye was measured in response to a 1 s light pulse ranging between 13.0 and 15.7 log quanta.cm^{-2}.s^{-1}. The 409 nm LED had a maximum irradiance of 0.00015 W.cm^{-2} at 14.6 log quanta.cm^{-2}.s^{-1}. This is equivalent to a stimulus luminance of 9.64 cd.m^{-2} (the retinal illuminance in Trolands for an 8.0 mm pupil is 484.56 Td). The maximum output of the LED is therefore below the upper exposure limits (0.003 W.cm^{-2}) to prevent any phototoxicity from UV radiation.[31] The wavelength of successive test stimuli was always greater than 100 nm to control for melanopsin bistability.[5] The criterion PIPR amplitude was defined as 8% for the plateau PIPR, 10% for the 6 s PIPR, 4 log units for the AUC Early and AUC Late. The retinal irradiances required at each wavelength to produce the criterion PIPR were normalized and fitted with a vitamin A1 pigment nomogram.[32]

The PLR was measured with the Maxwellian view optical system at two wavelengths [short wavelength: λ_{max} = 465 nm (bluish); long wavelength: λ_{max} = 637 nm (reddish)] over a 5 log

148 unit range of retinal irradiances to span low to high melanopsin excitation levels [9.8-14.8 log
149 quanta.cm^{-2}.s^{-1} (-2.0 to 2.8 log cd.m^{-2} luminance) for the 465 nm light; 9.9-14.9 log
150 quanta.cm^{-2}.s^{-1} (-2.3 to 2.8 log cd.m^{-2} luminance) for the 637 nm light]. Figure 1 shows the
151 temporal sequence of the pupillometry protocols. Three stimulus durations (1 s, 10 s, and
152 30 s) were chosen to reflect the durations commonly adopted in published protocols. The 1 s
153 duration pulse was chosen because the 6 s and net 6 s PIPR amplitudes are largest with 1 s
154 pulses.[17] The 10 s pulse has been widely used in clinical studies of the PIPR but only three
155 different parameters have been quantified (redilation velocity, plateau, and 6 s PIPR).[8, 12, 13, 17,
156 21-24] The 30 s pulse was studied because ipRGCs dominate the steady-state pupil response
157 during light presentation compared to rod and cone inputs when stimulus durations are
158 > 10 s.[13] All irradiances were above rod threshold.[33] Retinal irradiances are photopic when
159 > 11.8 log quanta.cm^{-2}.s^{-1}.[11] The pre-stimulus duration was 10 s for all conditions. The post-
160 stimulus recording period ranged from 40 to 600 s to ensure that the sustained
161 pupilloconstriction returned to baseline before re-measurement. Pilot studies determined that
162 the inter-stimulus interval (ISI) for return to baseline to be between 100 and 660 s; the ISI
163 increased with increasing retinal irradiance and stimulus duration. To consider the effect of
164 dilation of the stimulated eye on the PIPR of the fellow eye, a subset of two participants
165 underwent pilot testing with their right eye dilated with 1% Tropicamide (Minims, Chauvin
166 Pharmaceuticals Ltd., England). There was < 4% coefficient of variation (CV) between the
167 metrics for the undilated and dilated conditions, within the acceptable range of CV (see
168 'Statistical Analysis' for details on CV). Since there is evidence of unequal consensual and
169 direct PLR in some normal persons,[34] we compared the metrics between the consensual and
170 direct PLR in these two participants and found < 7% CV for our test protocols.

171 All measurements were preceded by 10 minutes dark adaptation in a darkened (< 1 lux)
172 laboratory. For the PLR measurements, short and long wavelength stimulus lights were
173 alternated in all sessions to control for the effect of melanopsin bistability.[5] Every
174 measurement for each stimulus wavelength, irradiance, and duration combination was

repeated at least three times with the time interval equal to the corresponding ISI. Table 1 specifies the individual photoreceptor excitations for the stimuli;[35] the L-cones, M-cones, and rods have higher sensitivity to the 637 nm light than melanopsin or S-cones, whereas melanopsin, rods, and S-cones have higher sensitivity to the 465 nm light compared to the L-cones or M-cones. It should be noted that narrow band lights do not provide photoreceptor isolation and that the high (or low) photoreceptor excitations specified in Table 1 do not imply that a photoreceptor does (or does not) contribute to the PLR; these factors depend on the relative contributions of these photoreceptors inputs to the pupil pathway and their variation with the stimulus properties (e.g., spatial, temporal, and wavelength), of which many of these factors are unknown.

Table 1. Individual photoreceptor excitation (in $\log_{10}$ units) with 465 nm and 637 nm light stimuli at different retinal irradiances (Based on Lucas et al[35]).

Photo-receptor Excitation	**α-opic lux (log units)**											
	9.8 log quanta.cm^{-2}.s^{-1}		10.8 log quanta.cm^{-2}.s^{-1}		11.8 log quanta.cm^{-2}.s^{-1}		12.8 log quanta.cm^{-2}.s^{-1}		13.8 log quanta.cm^{-2}.s^{-1}		14.8 log quanta.cm^{-2}.s^{-1}	
	465 nm	*637 nm*	*465 nm*	*637 nm*	*465 nm*	*637 nm*	*465 nm*	*637 nm*	*465 nm*	*637 nm*	*465 nm*	*637 nm*
S cone	-1.6	-7.9	-0.6	-6.9	0.4	-5.9	1.4	-4.9	2.4	-3.9	3.4	-2.9
Melanopsin	-1.8	-5.2	-0.8	-4.2	0.2	-3.2	1.2	-2.2	2.2	-1.2	3.2	-0.2
Rod	-1.9	-4.4	-0.9	-3.4	0.1	-2.4	1.1	-1.4	2.1	-0.4	3.1	0.6
M cone	-2.3	-3.0	-1.2	-2.0	-0.3	-1.0	0.8	0.0	1.8	1.0	2.8	2.0
L cone	-2.6	-2.3	-1.3	-1.3	-0.6	-0.3	0.4	0.7	1.4	1.7	2.4	2.7

Because the shape of the pupil image is elliptical when measured during off-axis fixation,[36] we determined that estimated pupil diameter measured in our Maxwellian view optical system would be underestimated by 0.113 ± 0.024 mm when the fixation eccentricity was up to 8.13º off-axis. For all pupil recordings used in the analysis, the eye movements were within 5˚ of central fixation axis of the optical system and IR camera plane, introducing an error of ≤ 0.07 mm in estimated pupil diameter.

Analysis of the Pupil Light Reflex (PLR) and Post-illumination Pupil Response (PIPR)

The PLR and PIPR were described by the 12 metrics outlined in Table 2 and Figure 2. The metrics were derived from the best-fit of the linear and exponential model to the data.[8, 14, 21, 22] For the peak constriction amplitude, 6 s PIPR, and plateau PIPR, a smaller value indicates a larger pupil response. Larger PIPR amplitudes are defined by smaller values of the redilation velocity, 6 s PIPR, and plateau PIPR; and larger values of the AUC early and late and PIPR duration. Though the models yield negative values for pupil dynamics, absolute values are used in Figures.

Table 2. Description and definition of the PLR metrics during light stimulation and PIPR metrics after light offset

	Metrics	***Definition and Units***
	Baseline pupil diameter (BPD)	Average 10 s pre-stimulus period (mm)
	Transient PLR	Peak % change from 180 – 500 ms after light onset[19, 22]
PLR metrics	PLR latency	Time (s) for 1% constriction
	Constriction velocity	Stimulus gradient of linear model ($mm.s^{-1}$) at light onset
	Peak constriction amplitude	Minimum pupil size (% baseline) during light presentation
	Time to peak	Time (s) to peak pupil constriction
	Pupil escape	Stimulus gradient of linear model ($mm.s^{-1}$) during light stimulation
PIPR metrics	Redilation velocity	Global rate constant (k) of exponential model ($mm.s^{-1}$)[8, 21]
	6 s PIPR amplitude	Pupil size (% baseline) at 6 s after light offset[8, 17, 21]
	Plateau PIPR	Plateau of exponential model (% baseline)[21]
	AUC early	$\sum$ (BPD - APD)* over 0-10 s after light offset[18] (unitless)
	AUC Late	$\sum$ (BPD - APD) over 10-30 s after light offset[18] (unitless)
	PIPR duration	Time (s) to return to baseline after light offset
	Net PIPR metrics	Difference between 465 nm and 637 nm PIPR[23, 24] (unit of corresponding metric)

*APD – Absolute pupil diameter

Statistical Analysis

Statistical data analysis was conducted using GraphPad Prism (GraphPad Software, Inc., CA, USA). Means ± standard deviation (SD) were used to describe data. Shapiro-Wilk tests indicated that all data were normally distributed. One-way repeated measures ANOVA (95% confidence interval, $p < 0.05$, Turkey's test for pairwise multiple comparisons, Geisser-Greenhouse correction) was applied to compute the differences in the pupil responses between different stimulus durations. To determine variability of the PIPR and net PIPR metrics the intra and inter-individual coefficient of variation (CV) was calculated (SD/mean). The CV provides a more precise measurement of variability than SD because it is dimensionless and is not affected by changes in measurement units.[37] A CV ≤ 0.2 was considered acceptable based on the target acceptance criteria for immunoassay applications;[38, 39] we are unaware of a literature reference for a CV for human behavioural studies.

RESULTS

The spectral sensitivity of the PIPR metrics is shown in Figure 3 for the two observers (circle and square symbols). The data for all metrics (plateau, 6 s, early and late AUC) are well described by a Vitamin A1 nomogram with a peak spectral sensitivity at 482 nm. There were no differences in spectral sensitivity derived from the modelled data (shown) and the raw unmodeled data (not shown).

The PLR during light stimulation and the PIPR after light offset were analyzed using twelve metrics (Table 2) as described in the following sections for the group data. Figure 4 shows the complete PLR data for one representative participant. While the PLR response is not the primary outcome of this study, it is presented before the PIPR results to follow the natural time sequence during and after light stimulation.

Effect of Stimulus Irradiance, Wavelength, and Duration on the PLR

Figure 5 reports the mean group data across all stimulus irradiances and shows that with increasing irradiance, the transient PLR increased and the PLR latency shortened with a plateau beyond 12.8 log quanta.cm^{-2}.s^{-1}. The constriction velocity and peak constriction amplitude increased, whereas the time to peak constriction and pupil escape did not change as a function of irradiance. The effect of stimulus duration on the PLR was wavelength and irradiance dependent. The transient PLR was independent of stimulus duration [465 nm: $F_{2,7}$ = 1.378, p = 0.298; 637 nm: $F_{2,10}$ = 0.52, p = 0.607] and so was PLR latency [465 nm: $F_{2,8}$ = 3.89, p = 0.069; 637 nm: $F_{2,7}$ = 2.15, p = 0.187]. However, the transient PLR amplitude was always larger and the PLR latency was shorter for short wavelengths than for long wavelengths due to higher rod sensitivity, but this difference tapered with increasing irradiance showing saturation of the response. When the data were normalized to peak pupil constriction, the PLR latency still showed a trend of shortening with increasing irradiance indicating that this process is driven by stimulus irradiance. The constriction velocity was dependent on stimulus duration at short wavelengths [465 nm: $F_{1,7}$ = 26.24, p = 0.001] and was faster for 30 s stimuli than 1 s and 10 s stimuli, but independent of duration at long wavelengths [637 nm: $F_{2,8}$ = 0.17, p = 0.805]. The peak constriction amplitude increased with increasing stimulus duration [465 nm: $F_{1,6}$ = 26.88, p = 0.002; 637 nm: $F_{1,6}$ = 7.97, p = 0.025]. The time to peak constriction was longer for 30 s and 10 s pulses than for 1 s pulses [465 nm: $F_{2,7}$ = 26.66, p = 0.001; 637 nm: $F_{2,10}$ = 7.73, p = 0.010]; for 1 s pulses, the time to peak constriction was longer for 465 nm (1.4 to 1.9 s) than 637 nm (1.2 to 1.4 s) above 11.8 log quanta.cm^{-2}.s^{-1} indicating a slower temporal response to the short wavelength stimuli. The pupil escape velocity was independent of stimulus irradiance, but dependent on stimulus duration [465 nm: $F_{1,5}$ = 20.33, p = 0.006; 637 nm: $F_{1,5}$ = 7.97, p = 0.017], with a slower escape with 30 s pulses than 10 s pulses (note that escape velocity is not applicable to 1 s pulses).

Effect of Stimulus Irradiance, Wavelength, and Duration on the PIPR

Figure 6 displays the effect of stimulus irradiance, wavelength and duration on the six PIPR metrics. The PIPR redilation velocity decreased with increasing irradiance for 1 s pulses, but was independent of irradiance for 10 s and 30 s pulses. At 465 nm, a second redilation phase (Figure 4) was observed at around 40, 50, and 70 s post-stimulus for 1, 10, and 30 s pulses at 14.8 log quanta.cm^{-2}.s^{-1} and which has not been previously reported. The 6 s PIPR, plateau PIPR, AUC early, AUC late, and PIPR duration increased with increasing stimulus irradiance. At the highest measured retinal irradiance (14.8 log quanta.cm^{-2}.s^{-1}), all PIPR metrics (except PIPR duration) for 1 s pulses were larger or equal to those for 10 s and 30 s pulses.

Redilation velocity was dependent on stimulus duration at long wavelengths, with higher redilation velocity for 1 s pulses than 10 s or 30 s pulses [637 nm: $F_{1,7} = 37.82$, $p = 0.0003$], but no effect at short wavelengths [465 nm: $F_{1,6} = 1.48$, $p = 0.278$]. Stimulus duration had no significant effect on the 6 s PIPR amplitude [465 nm: $F_{1,5} = 1.63$, $p = 0.258$; 637 nm: $F_{1,6} = 5.34$, $p = 0.052$], plateau PIPR amplitude [465 nm: $F_{1,5} = 2.81$, $p = 0.752$; 637 nm: $F_{2,7} = 0.38$, $p = 0.633$], AUC early [465 nm: $F_{2,10} = 3.06$, $p = 0.094$; 637 nm: $F_{2,7} = 8.05$, $p = 0.019$], AUC late [465 nm: $F_{1,7} = 1.25$, $p = 0.323$; 637 nm: $F_{2,10} = 0.79$, $p = 0.479$], and PIPR duration [465 nm: $F_{1,6} = 2.04$, $p = 0.210$; 637 nm: $F_{1,6} = 5.35$, $p = 0.062$]. However, at 14.8 log quanta.cm^{-2}.s^{-1}, the PIPR duration increased with increasing stimulus duration.

Figure 7 shows as expected, that the net PIPR for irradiances below melanopsin threshold was not significant for the three stimulus durations. Beyond 11.8 log quanta.cm^{-2}.s^{-1}, which is known to be within the melanopsin range,[11] all net PIPR metrics except the net redilation velocity for 10 s and 30 s pulses increased with increasing irradiance. There was no significant effect of stimulus duration on the net 6 s PIPR [$F_{1,6} = 4.72$, $p = 0.068$], net plateau PIPR [$F_{1,6} = 2.41$, $p = 0.174$], net AUC late [$F_{1,6} = 3.98$, $p = 0.094$], and net PIPR duration [$F_{1,6} = 0.29$, $p = 0.635$]. The net redilation velocity [$F_{1,6} = 11.57$, $p = 0.016$] and net AUC

early [$F_{1,6} = 7.93$, $p = 0.028$] were dependent on stimulus duration, with net velocity and net AUC larger for 1 s pulses than 10 s and 30 s pulses.

Intra and Inter-individual CV

To quantify the level of dispersion in the PIPR metrics, we calculated the coefficient of variation (Figure 8) and applied a criterion of ≤ 0.2.[38, 39] The intra-individual CV for the plateau PIPR and 6 s PIPR was ≤ 0.2 with the others > 0.2 at all measured irradiances. The inter-individual CV of the PIPR in the melanopsin range was ≤ 0.2 for the plateau PIPR, 6 s PIPR, and AUC early and late recovery whereas the CV was > 0.2 for all other PIPR metrics.

DISCUSSION

This study shows a nomogram at the peak sensitivity of the melanopsin (opn4) photopigment (λ_{max} = 482 nm) adequately describes the spectral sensitivity derived from all current PIPR metrics and thus any of these metrics can be used to quantify the PIPR to obtain a measure of the intrinsic melanopsin photoresponse. The PIPR amplitude and intra and inter-individual variability is stimulus dependent. The largest PIPR amplitude was obtained with a 1 s short wavelength pulse (retinal irradiance ≥ 12.8 log quanta.cm^{-2}.s^{-1}) and the intra and inter-individual variability was lowest for the 6 s and plateau PIPR metrics. Of the test stimuli and six PIPR metrics evaluated, we propose that 1 s stimuli and the plateau and/or 6 s PIPR metrics will be most applicable for clinical studies of ipRGC function. We further observed that the maximum duration of the sustained PIPR was 83 s for 1 s pulses and 180 s for 30 s pulses (465 nm; 14.8 log quanta.cm^{-2}.s^{-1}), but there is large intra and inter-individual variation.

Post-illumination Pupil Response (PIPR)

The PIPR amplitude was larger with 1 s pulses than with 10 s, which is larger than with 30 s pulses for retinal irradiances ≥ 12.8 log quanta.cm^{-2}.s^{-1}, as evident in the comparison between

311 1 s and 30 s pulses[9] and 1 s and 10 s pulses.[17] This duration dependent response amplitude
312 may be due to the peak ipRGC firing, with stimuli longer than 1 s, occurring 2-3 s after
313 stimulus onset and then gradually decaying[11, 26, 40] with light adaptation.[41] Together this may
314 lead to the lower PIPR amplitude observed with longer stimulus durations. However, with
315 14.8 log quanta.cm^{-2}.s^{-1}, 465 nm pulses, the PIPR duration increases with increasing stimulus
316 duration from 1 s to 30 s, in agreement with a study in mouse eyes[42] that showed the duration
317 of the PIPR increased with stimulus duration from 50 ms to 1 s, possibly due to increased
318 light adaptation of melanopsin signaling over time.

319 One study[18] reported only the test-retest repeatability of the AUC early (Intra-class
320 Correlation Coefficient, ICC = 0.6) and late recovery (ICC = 0.8) and another study[43] reported
321 variation of the plateau PIPR metric (CV = 0.16, ICC = 0.95, 30° central stimulus) but no
322 other metrics. We report the intra and inter-individual variability of all current PIPR metrics.
323 Another study reported a lower inter-individual coefficient of variation for the 6 s PIPR than
324 the plateau PIPR,[44] whereas our study showed a low CV (≤ 0.2) for both 6 s and plateau PIPR
325 metrics compared to all other metrics. However, that study used a larger stimulus (60˚x90˚)
326 and defined the plateau PIPR as the average PIPR from 10-30 s post-stimulus, hence it may
327 not be comparable to our results. In our study with a smaller central stimulus field (35.6˚), the
328 PIPR variability increased with increasing irradiance, indicating that at higher irradiances a
329 larger PIPR can be produced, but with larger variability. Lei et al[43, 44] showed a lower
330 variation in PIPR at higher irradiances with large stimuli (full-field and 60˚x90˚) probably
331 because the mass response from ipRGCs at high irradiances with large field stimulation
332 reduces the inter-individual variability. It is known that the pupil constriction amplitudes to
333 large stimuli are greater than to smaller stimuli of equal irradiance.[1] For a constant corneal
334 flux density, the pupil constriction amplitude is independent of stimulus size.[45, 46] With
335 regards to the effect of stimulus size on the PIPR, full-field stimuli presented in Newtonian
336 view produce a larger sustained PIPR with less variability than smaller central-field (60˚x90˚
337 & 30˚) and hemi-field (half of 30˚ central-field) stimuli.[43, 44] Larger stimuli however will be

less sensitive to early local retinal deficits (see Feigl & Zele., 2014 for review).[28] Studies in mouse models have indicated that ipRGCs are robust to axonal injury[47, 48] and induced chronic ocular hypertension.[49] Studies in mouse models of retinal degeneration suggest that ipRGC axons/dendrites remain unaffected in early stages and ipRGC density conserves until the advanced stages of retinal degeneration.[50,51] Further work is required to understand the role of redundancy and robustness of ipRGCs during disease in humans to define the complex relationships between ipRGC dysfunction and PIPR amplitude, dynamics, and variability of the response.

We determined that the PIPR duration is longer (> 83.4 ± 48.0 s) than previously reported[8, 12, 14, 17-19, 21-23] and subsequently, longer than the ISI employed in many studies. The ISI should vary with stimulus irradiance because the PIPR duration increases with increasing irradiance and the *in vitro* intrinsic response also scales with irradiance in melanopsin excitation range.[52] Based on our measurements we propose that for 1 s short wavelength pulses ≥ 14.8 log quanta.cm^{-2}.s^{-1}, the inter-stimulus interval (ISI) should be at least 83 s (95% CI: Upper: 159.8 s), so that the sustained PIPR does not interfere with subsequent recordings. The PIPR durations were longer for 1 s than 10 s and 30 s pulses at 12.8 and 13.8 log quanta.cm^{-2}.s^{-1} possibly indicating different adaptation responses to the stimulus durations. Finally, by measuring the PIPR at high irradiances we observed that the post-stimulus pupil redilation shows two phases (Figure 4; first phase just after light offset and second phase at about 40, 50, and 70 s post-stimulus for 1, 10, and 30 s pulses), with the latter phase for short wavelength pulses at 14.8 log quanta.cm^{-2}.s^{-1} not well described by a single exponential function. While the origin of this biphasic redilation is not clear, it may reflect different adaptation processes or the contribution of different ipRGC subtypes.[53-55]

Pupil Light Reflex (PLR) during Light Stimulation

Analysis of the PLR metrics during light stimulation indicates that the time to peak constriction is longer for 465 nm than 637 nm with 1 s pulses in melanopsin range whereas

this difference was not present below melanopsin threshold. The time to peak constriction did not differ between 465 nm and 637 nm with 10 and 30 s pulses, in agreement with Tsujimura and Tokuda.[56] Pupil escape has been considered previously in detail by Loewenfeld,[1] Kardon et al.,[19] and McDougal and Gamlin.[13] In an extension to their observations, we found that pupil escape with 30 s pulses ($\geq$ 12.0 log quanta.cm^{-2}.s^{-1}) was slower than with 10 s pulses which we infer is due to larger relative ipRGC contributions to the steady-state pupil constriction,[13, 57] a decay in rod-cone response with stimuli longer than 10 s,[13] and ipRGC adaptation to steady light stimulation.[41] Together these markers indicate signature contributions of melanopsin to the pupil constriction amplitude and escape.

In general, the metrics quantifying the human PLR during light stimulation are in accordance with previous studies using different test stimulus protocols with broadband light stimuli. We found that the pupil constriction velocity is wavelength dependent; with long wavelengths, the velocity is independent of stimulus duration, as per the early findings of Lowenstein and Loewenfeld[58] who used broadband lights, whereas the constriction velocity to the short wavelength light was duration dependent, with the fastest velocity with 30 s pulses. The wavelength dependent effect on constriction velocity may be related to the differential rod and cone sensitivity to the wavelength and mediated extrinsically via ipRGCs.[13] Consistent with previous studies,[43, 44] pupil constriction velocity increased with increasing stimulus irradiance.[58, 59] Our findings confirm for narrow band lights that with increasing retinal irradiance, the magnitude of pupil constriction increases[58-61] and that the transient PLR increases and the PLR latency shortens.[19, 59, 62] The pupil attains the minimum latent period[1] at ~12.8 log quanta.cm^{-2}.s^{-1} indicating that the additional time delay of the PLR originating in the photoreceptors and neural reflex circuit and dependent on stimulus intensity,[1] is absent at 12.8 log quanta.cm^{-2}.s^{-1}, so the minimum latent period cannot be eliminated by further increases in stimulus intensity because the time delay is then limited by iris sphincter muscle strength.[1]

In a pilot experiment (n = 2), the PLR to a 1 s pulse (14.8 log quanta.cm^{-2}.s^{-1}) of undilated and dilated eyes were compared using the same metrics for describing the response as in the main experiment; we found < 4% coefficient of variation between two conditions. This is not surprising as we used a Maxwellian view pupillometer to provide an open-loop feedback.[1, 63] Further studies need to show whether a full field system using Newtonian stimulation[64] (closed-loop feedback) detects a difference between stimulated eyes with dilated and undilated pupils. We conclude that for a Maxwellian system, dilation of stimulated eye is not essential unless it is required to minimize accommodative fluctuations on pupil, or persons whose natural pupil diameter is small.

In conclusion, we propose that the PIPR produced by short duration pulses (e.g., ≤ 1s) with an irradiance above melanopsin threshold and described with the plateau and/or 6 s PIPR metrics may be the optimum protocol for monitoring disease progression in clinical studies of ipRGCs because short duration stimuli produce larger PIPR amplitudes and these two metrics show the least intra-individual coefficient of variation.

Acknowledgments: Supported by Australian Research Council Discovery Projects (ARC-DP140100333) to BF and AJZ. We thank Daniel S. Joyce for contributions to data collection.

REFERENCES

1. Loewenfeld I. *The Pupil: Anatomy, Physiology and Clinical Applications.* Boston: Butterworth-Heinemann; 1999;1:83-273.
2. Lucas RJ, Douglas RH, Foster RG. Characterization of an ocular photopigment capable of driving pupillary constriction in mice. *Nat Neurosci.* 2001;4:621-626.
3. Lucas R, Hattar S, Takao M, Berson D, Foster R, Yau KW. Diminished pupillary light reflex at high irradiances in melanopsin-knockout mice. *Science.* 2003;299:245-247.
4. Dacey DM, Peterson BB, Robinson FR, Gamlin PD. Fireworks in the primate retina: In vitro photodynamics reveals diverse LGN-projecting ganglion cell types. *Neuron.* 2003;37:15-27.
5. Mure LS, Rieux C, Hattar S, Cooper HM. Melanopsin-dependent nonvisual responses: Evidence for photopigment bistability in vivo. *J Biol Rhythms.* 2007;22:411-424.
6. Morin LP, Blanchard JH, Provencio I. Retinal ganglion cell projections to the hamster suprachiasmatic nucleus, intergeniculate leaflet, and visual midbrain: Bifurcation and melanopsin immunoreactivity. *J Comp Neurol.* 2003;465:401-416.
7. Hattar S, Lucas RJ, Mrosovsky N, et al. Melanopsin and rod–cone photoreceptive systems account for all major accessory visual functions in mice. *Nature.* 2003;424:75-81.
8. Zele AJ, Feigl B, Smith SS, Markwell EL. The circadian response of intrinsically photosensitive retinal ganglion cells. *PLoS One.* 2011;6:e17860.
9. Münch M, Léon L, Crippa SV, Kawasaki A. Circadian and wake-dependent effects on the pupil light reflex in response to narrow-bandwidth light pulses. *Invest Ophthalmol Vis Sci.* 2012;53:4546-4555.
10. Roecklein KA, Wong PM, Franzen PL, et al. Melanopsin gene variations interact with season to predict sleep onset and chronotype. *Chronobiol Int.* 2012;29:1036-1047.

11. Dacey DM, Liao HW, Peterson BB, et al. Melanopsin-expressing ganglion cells in primate retina signal colour and irradiance and project to the LGN. *Nature.* 2005;433:749-754.

12. Gamlin PDR, McDougal DH, Pokorny J, Smith VC, Yau KW, Dacey DM. Human and macaque pupil responses driven by melanopsin-containing retinal ganglion cells. *Vision Res.* 2007;47:946-954.

13. McDougal DH, Gamlin PD. The influence of intrinsically-photosensitive retinal ganglion cells on the spectral sensitivity and response dynamics of the human pupillary light reflex. *Vision Res.* 2010;50:72-87.

14. Markwell EL, Feigl B, Zele AJ. Intrinsically photosensitive melanopsin retinal ganglion cell contributions to the pupillary light reflex and circadian rhythm. *Clin Exp Optom.* 2010;93:137-149.

15. Barrionuevo PA, Nicandro N, McAnany JJ, Zele AJ, Gamlin P, Cao D. Assessing rod, cone and melanopsin contributions to human pupil flicker responses. *Invest Ophthalmol Vis Sci.* 2014;55:719-727.

16. Gooley JJ, Lu J, Chou TC, Scammell TE, Saper CB. Melanopsin in cells of origin of the retinohypothalamic tract. *Nat Neurosci.* 2001;4:1165-1165.

17. Park JC, Moura AL, Raza AS, Rhee DW, Kardon RH, Hood DC. Toward a clinical protocol for assessing rod, cone, and melanopsin contributions to the human pupil response. *Invest Ophthalmol Vis Sci.* 2011;52:6624-6635.

18. Herbst K, Sander B, Milea D, Lund-Andersen H, Kawasaki A. Test–retest repeatability of the pupil light response to blue and red light stimuli in normal human eyes using a novel pupillometer. *Front Neurol.* 2011;2:10.

19. Kardon R, Anderson SC, Damarjian TG, Grace EM, Stone E, Kawasaki A. Chromatic pupil responses: Preferential activation of the melanopsin-mediated versus outer photoreceptor-mediated pupil light reflex. *Ophthalmology.* 2009;116:1564-1573.

20. Kardon R, Anderson SC, Damarjian TG, Grace EM, Stone E, Kawasaki A. Chromatic pupillometry in patients with retinitis pigmentosa. *Ophthalmology.* 2011;118:376-381.

21. Feigl B, Mattes D, Thomas R, Zele AJ. Intrinsically photosensitive (melanopsin) retinal ganglion cell function in glaucoma. *Invest Ophthalmol Vis Sci.* 2011;52:4362-4367.

22. Feigl B, Zele AJ, Fader SM, et al. The post-illumination pupil response of melanopsin-expressing intrinsically photosensitive retinal ganglion cells in diabetes. *Acta Ophthalmol.* 2012;90:230-234.

23. Kankipati L, Girkin CA, Gamlin PD. Post-illumination pupil response in subjects without ocular disease. *Invest Ophthalmol Vis Sci.* 2010;51:2764-2769.

24. Kankipati L, Girkin CA, Gamlin PD. The post-illumination pupil response is reduced in glaucoma patients. *Invest Ophthalmol Vis Sci.* 2011;52:2287-2292.

25. Joyce DS, Feigl B, Cao D, Zele AJ. Temporal characteristics of melanopsin inputs to the human pupil light reflex. *Vision Res.* 2015;107:58-66.

26. Wong KY. A retinal ganglion cell that can signal irradiance continuously for 10 hours. *J Neurosci.* 2012;32:11478-11485.

27. Nissen C, Sander B, Milea D, et al. Monochromatic pupillometry in unilateral glaucoma discloses no adaptive changes subserved by the ipRGCs. *Front Neurol.* 2014;5:15.

28. Feigl B, Zele AJ. Melanopsin-expressing intrinsically photosensitive retinal ganglion cells in retinal disease. *Optom Vis Sci*. 2014;91:894-903.

29. Kawasaki A, Munier FL, Leon L, Kardon RH. Pupillometric quantification of residual rod and cone activity in Leber congenital amaurosis. *Arch Ophthalmol.* 2012;130:798-800.

30. Beer RD, MacLeod DI, Miller TP. The extended maxwellian view (bigmax): A high-intensity, high-saturation color display for clinical diagnosis and vision research. *Behav Res Methods.* 2005;37:513-521.

493 31. Protection ICoN-IR. Guidelines on limits of exposure to ultraviolet radiation of
494 wavelengths between 180 nm and 400 nm (incoherent optical radiation). *Health*
495 *Physics.* 2004;87:171-186.
496 32. Dartnall H. The interpretation of spectral sensitivity curves. *Br Med Bull.* 1953;9:24-
497 30.
498 33. Zele AJ, Cao D. Vision under mesopic and scotopic illumination. *Front Psychol.*
499 2014;5:1594.
500 34. Smith S, Ellis C, Smith S. Inequality of the direct and consensual light reflexes in
501 normal subjects. *Br J Ophthalmol.* 1979;63:523-527.
502 35. Lucas RJ, Peirson SN, Berson DM, et al. Measuring and using light in the melanopsin
503 age. *Trends Neurosci.* 2014;37:1-9.
504 36. Mathur A, Gehrmann J, Atchison DA. Pupil shape as viewed along the horizontal
505 visual field. *J Vis.* 2013;13:3.
506 37. Reed GF, Lynn F, Meade BD. Use of coefficient of variation in assessing variability
507 of quantitative assays. *Clin Diagn Lab Immunol.* 2002;9:1235-1239.
508 38. Findlay J, Smith W, Lee J, et al. Validation of immunoassays for bioanalysis: A
509 pharmaceutical industry perspective. *J Pharm Biomed Anal.* 2000;21:1249-1273.
510 39. Shah VP, Midha KK, Findlay JW, et al. Bioanalytical method validation—a revisit
511 with a decade of progress. *Pharm Res.* 2000;17:1551-1557.
512 40. Wong KY, Dunn FA, Berson DM. Photoreceptor adaptation in intrinsically
513 photosensitive retinal ganglion cells. *Neuron.* 2005;48:1001-1010.
514 41. Do MTH, Yau KW. Adaptation to steady light by intrinsically photosensitive retinal
515 ganglion cells. *Proc Natl Acad Sci.* 2013;110:7470-7475.
516 42. Vugler A, Semo M, Ortín-Martínez A, et al. A role for the outer retina in development
517 of the intrinsic pupillary light reflex in mice. *Neuroscience.* 2015;286:60-78.
518 43. Lei S, Goltz HC, Chandrakumar M, Wong AM. Test-retest reliability of hemifield,
519 central-field and full-field chromatic pupillometry for assessing the function of

melanopsin-containing retinal ganglion cells. *Invest Ophthalmol Vis Sci.* 2015;56:1267-1273.

44. Lei S, Goltz HC, Chandrakumar M, Wong AM. Full-field chromatic pupillometry for the assessment of the post-illumination pupil response driven by melanopsin-containing retinal ganglion cells. *Invest Ophthalmol Vis Sci.* 2014;55:4496-4503.

45. Atchison DA, Girgenti CC, Campbell GM, Dodds JP, Byrnes TM, Zele AJ. Influence of field size on pupil diameter under photopic and mesopic light levels. *Clin Exp Optom.* 2011;94:545-548.

46. Stanley PA, Davies AK. The effect of field of view size on steady-state pupil diameter. *Ophthalmic Physiol Opt.* 1995;15:601-603.

47. de Sevilla Müller LP, Sargoy A, Rodriguez AR, Brecha NC. Melanopsin ganglion cells are the most resistant retinal ganglion cell type to axonal injury in the rat retina. *PLoS One.* 2014;9:e93274.

48. Robinson G, Madison R. Axotomized mouse retinal ganglion cells containing melanopsin show enhanced survival, but not enhanced axon regrowth into a peripheral nerve graft. *Vision Res.* 2004;44:2667-2674.

49. Li RS, Chen BY, Tay DK, Chan HH, Pu ML, So KF. Melanopsin-expressing retinal ganglion cells are more injury-resistant in a chronic ocular hypertension model. *Invest Ophthalmol Vis Sci.* 2006;47:2951-2958.

50. Vugler AA, Semo M, Joseph A, Jeffery G. Survival and remodeling of melanopsin cells during retinal dystrophy. *Vis Neurosci.* 2008;25:125-138.

51. Esquiva G, Lax P, Cuenca N. Impairment of intrinsically photosensitive retinal ganglion cells associated with late stages of retinal degeneration. *Invest Ophthalmol Vis Sci.* 2013;54:4605-4618.

52. Berson DM, Dunn FA, Takao M. Phototransduction by retinal ganglion cells that set the circadian clock. *Science.* 2002;295:1070-1073.

53. Baver SB, Pickard GE, Sollars PJ, Pickard GE. Two types of melanopsin retinal ganglion cell differentially innervate the hypothalamic suprachiasmatic nucleus and the olivary pretectal nucleus. *Eur J Neurosci*. 2008;27:1763-1770.

54. Chen SK, Badea T, Hattar S. Photoentrainment and pupillary light reflex are mediated by distinct populations of ipRGCs. *Nature*. 2011;476:92-95.

55. Estevez ME, Fogerson PM, Ilardi MC, et al. Form and function of the M4 cell, an intrinsically photosensitive retinal ganglion cell type contributing to geniculocortical vision. *J Neurosci*. 2012;32:13608-13620.

56. Tsujimura S, Tokuda Y. Delayed response of human melanopsin retinal ganglion cells on the pupillary light reflex. *Ophthalmic Physiol Opt.* 2011;31:469-479.

57. Tsujimura S, Ukai K, Ohama D, Nuruki A, Yunokuchi K. Contribution of human melanopsin retinal ganglion cells to steady-state pupil responses. *Proc R Soc Lond B Biol Sci.* 2010;277:2485-2492.

58. Lowenstein O, Loewenfeld IE. *The eye* In: Davson H, ed. Vol 3. 2 ed: New York: Academic Press; 1969.

59. Ellis C. The pupillary light reflex in normal subjects. *Br J Ophthalmol.* 1981;65:754-759.

60. Moon P, Spencer DE. Visual data applied to lighting design. *J Opt Soc Am.* 1944;34:605-614.

61. Alpern M, McCready DW, Barr L. The dependence of the photopupil response on flash duration and intensity. *J Gen Physiol.* 1963;47:265-278.

62. Loewenfeld IE. Pupillary movements associated with light and near vision. *Recent Developments in Vision Research*. 1966:17.

63. Stark L, Sherman PM. A servoanalytic study of consensual pupil reflex to light. *J Neurophysiol.* 1957;20:17-26.

64. Burns SA, Webb RH. Optical generation of the visual stimulus. *Handbook of Optics, M Bass, EW van Stryland, DR Williams, and WL Wolfe, eds(McGraw-Hill, 1994).* 1994:1-28.

FIGURE LEGENDS

Figure 1. Temporal sequence of the stimulus protocol for the pupillometry experiments. Retinal irradiance is specified on the left ordinate and post-stimulus time on the abscissa. PRE = pre-stimulus period, Stimulus (3 durations, 30s: upper; 10s, 1s, lower), PIPR = Post Illumination Pupil Response, ISI = inter-stimulus interval.

Figure 2. An exemplar of the PLR and PIPR in response to a short wavelength (465 nm), 30s light pulse. The metrics used to quantify the pupil light response during and after light stimulation are indicated on the pupil trace and defined in Table 2. The blue trace indicates the PLR and PIPR; the gray trace shows the model.

Figure 3. Spectral sensitivity of the plateau PIPR, 6 s PIPR, AUC early and late recovery metrics. In each panel, the circles and squares indicate the data (average ± SD) from two participants. The data of 32/F observer are horizontally offset from 31/M observer by 3.5 nm. The solid blue lines indicate the vitamin A1 nomogram (λ_{max} = 482 nm), and the insets show the corresponding metrics. The legends in the first panel are common to all panels.

Figure 4. Average pupil response of a representative participant (30 year old female) to short (465 nm) and long wavelength (637 nm) stimuli of retinal irradiance between 9.8 to 14.8 log quanta.cm^{-2}.s^{-1} increasing in 1 log unit steps, and three durations: 1 s (Panel A), 10 s (B), and 30 s (C). The retinal irradiance is defined in log quanta.cm^{-2}.s^{-1} (with log Trolands given in parentheses) next to the corresponding pupil trace in the upper panels. Stimulus duration is indicated by the colored rectangular bar on the abscissa. Insets show the 30 s PIPR with the dotted vertical lines indicating the 6 s PIPR amplitude and gray lines indicating the models. All data are offset successively by 5% along the ordinates from the 9.8 log quanta.cm^{-2}.s^{-1} trace. The same color coding is followed in all panels.

Figure 5. Average (± SD) (n=5 participants) transient pupil light response (PLR) (%), PLR latency (ms), constriction velocity ($mm.s^{-1}$), peak constriction amplitude (% baseline), time to peak constriction (s), and pupil escape ($mm.s^{-1}$) of the PLR to stimuli of wavelength 465 nm (blue) and 637 nm (red), retinal irradiance between 9.8 to 14.8 log $quanta.cm^{-2}.s^{-1}$ increasing in 1 log unit steps, and three durations: 1 s (squares), 10 s (triangles), and 30 s (circles). The numbers in blue and red in the upper left and right panels indicate the luminance (log $cd.m^{-2}$) of the short and long wavelength stimuli respectively.

Figure 6. Average (±SD) (n=5) redilation velocity ($mm.s^{-1}$), 6 s PIPR amplitude ((% baseline), plateau PIPR ((% baseline), AUC early and late recovery (linear and log units), and PIPR duration (s) of the pupil light response to stimuli of wavelength 465 nm (blue) and 637 nm (red), retinal irradiance between 9.8 to 14.8 log $quanta.cm^{-2}.s^{-1}$ increasing in 1 log steps, and three durations: 1 s (squares), 10 s (triangles), and 30 s (circles). The numbers in blue and red in the upper left and right panels indicate the luminance (log $cd.m^{-2}$) of the short and long wavelength stimuli respectively.

Figure 7. Average (±SD) (n = 5) net redilation velocity (A), net 6 s PIPR (B), net plateau PIPR (C), net AUC early (D) and late (E) recovery, and net PIPR duration (F) of the pupil light response to stimuli of wavelength 465 nm and 637 nm, retinal irradiance from 9.8 to 14.8 log $quanta.cm^{-2}.s^{-1}$ increasing in 1 log steps, and three durations: 1 s (squares), 10 s (triangles), and 30 s (circles).

Figure 8. Intra-individual (upper two rows) and inter-individual (lower two rows) Coefficient of Variation (CV) of the PIPR metrics for short wavelength stimuli. The CVs for long wavelength stimuli (not shown) were similar. The traces joined by squares, triangles, and circles represent the data for 1 s, 10 s, and 30 s pulses in all panels. The data points with a CV >1.0 are not shown.

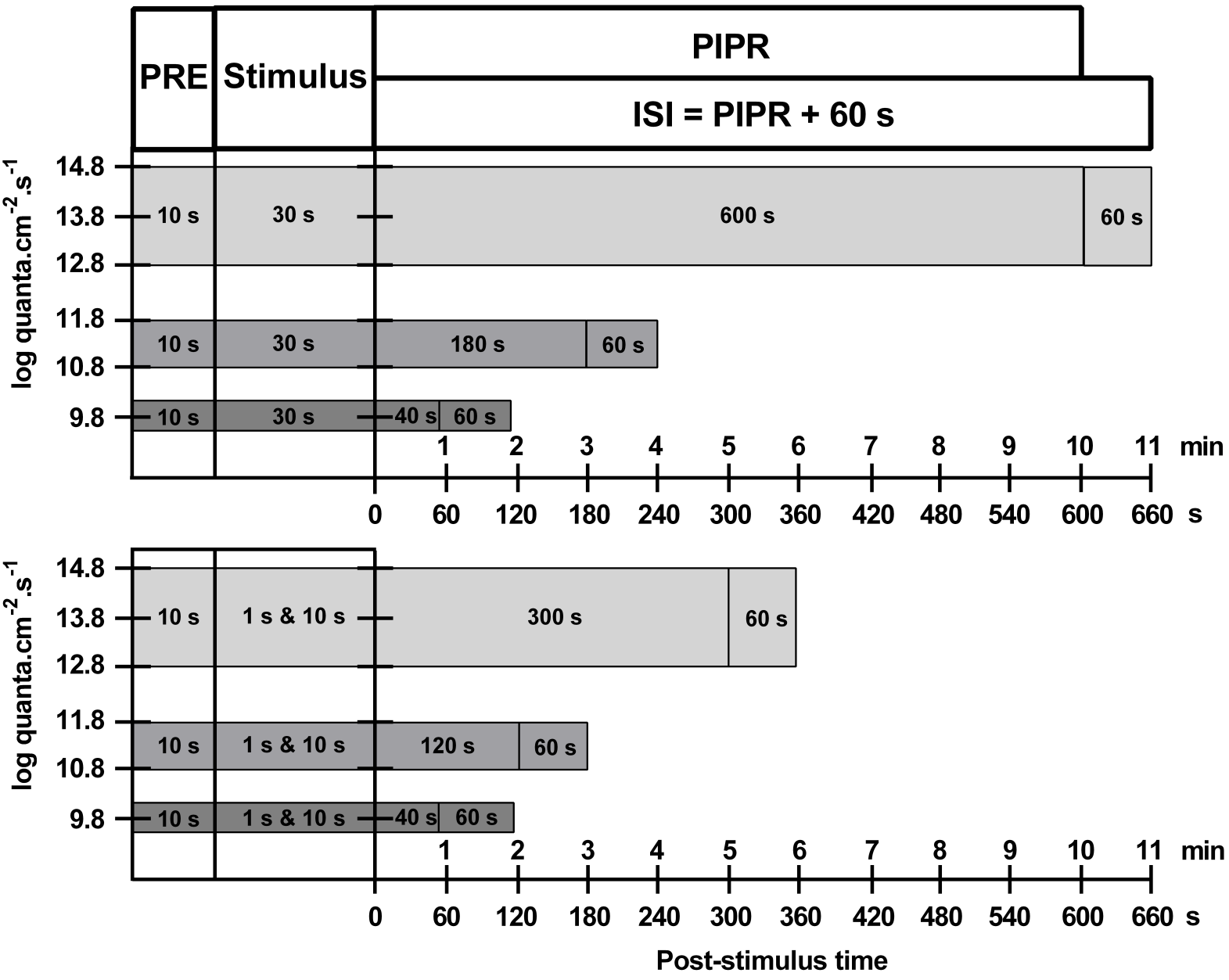
PRE
Stimulus
PIPR
ISI = PIPR + 60 s
log quanta.cm-2.s-1
14.8
13.8
12.8
11.8
10.8
9.8
10 s
30 s
600 s
60 s
10 s
30 s
180 s
60 s
10 s
30 s
40 s
60 s
1 2 3 4 5 6 7 8 9 10 11 min
0 60 120 180 240 300 360 420 480 540 600 660 s
log quanta.cm-2.s-1
14.8
13.8
12.8
11.8
10.8
9.8
10 s
1 s & 10 s
300 s
60 s
10 s
1 s & 10 s
120 s
60 s
10 s
1 s & 10 s
40 s
60 s
1 2 3 4 5 6 7 8 9 10 11 min
0 60 120 180 240 300 360 420 480 540 600 660 s
Post-stimulus time

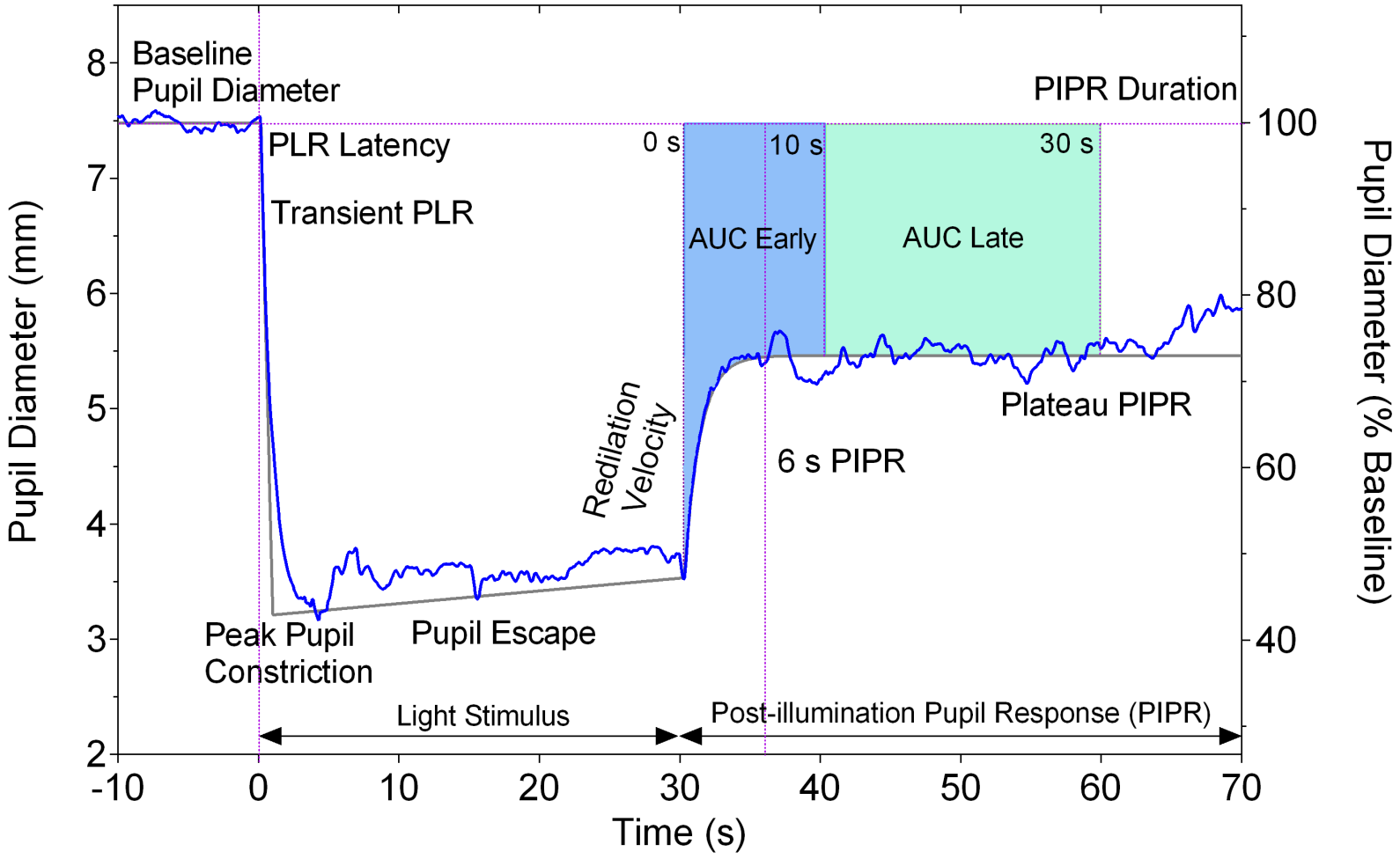
Baseline
Pupil Diameter
PLR Latency
Transient PLR
Peak Pupil
Constriction
Pupil Escape
Redilation
Velocity
0 s
10 s
30 s
AUC Early
AUC Late
6 s PIPR
Plateau PIPR
PIPR Duration
Light Stimulus
Post-illumination Pupil Response (PIPR)
Pupil Diameter (mm)
Pupil Diameter (% Baseline)
Time (s)
8
7
6
5
4
3
2
100
80
60
40
-10
0
10
20
30
40
50
60
70

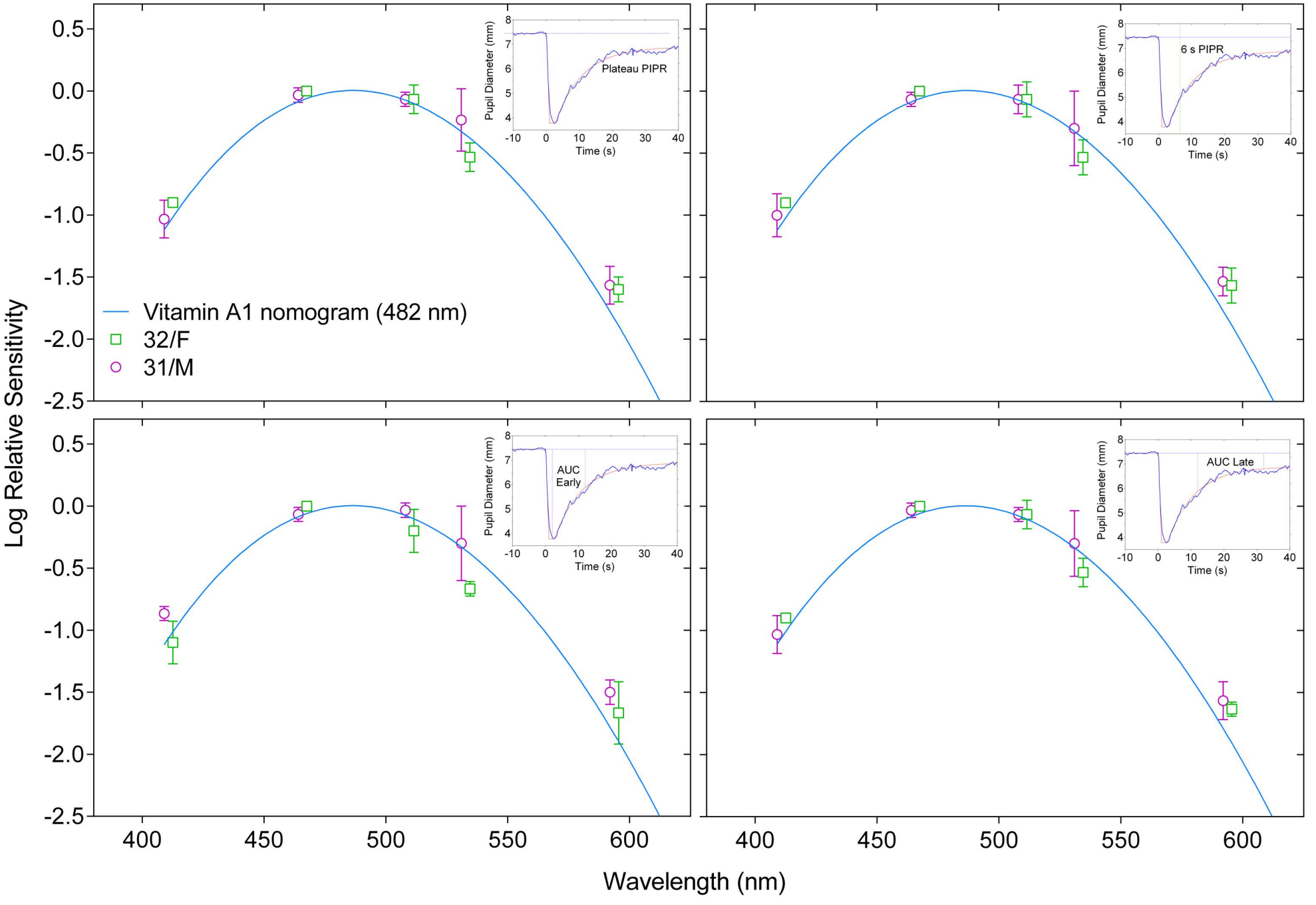
Log Relative Sensitivity
Wavelength (nm)
Vitamin A1 nomogram (482 nm)
32/F
31/M
Plateau PIPR
6 s PIPR
AUC Early
AUC Late
Pupil Diameter (mm)
Time (s)

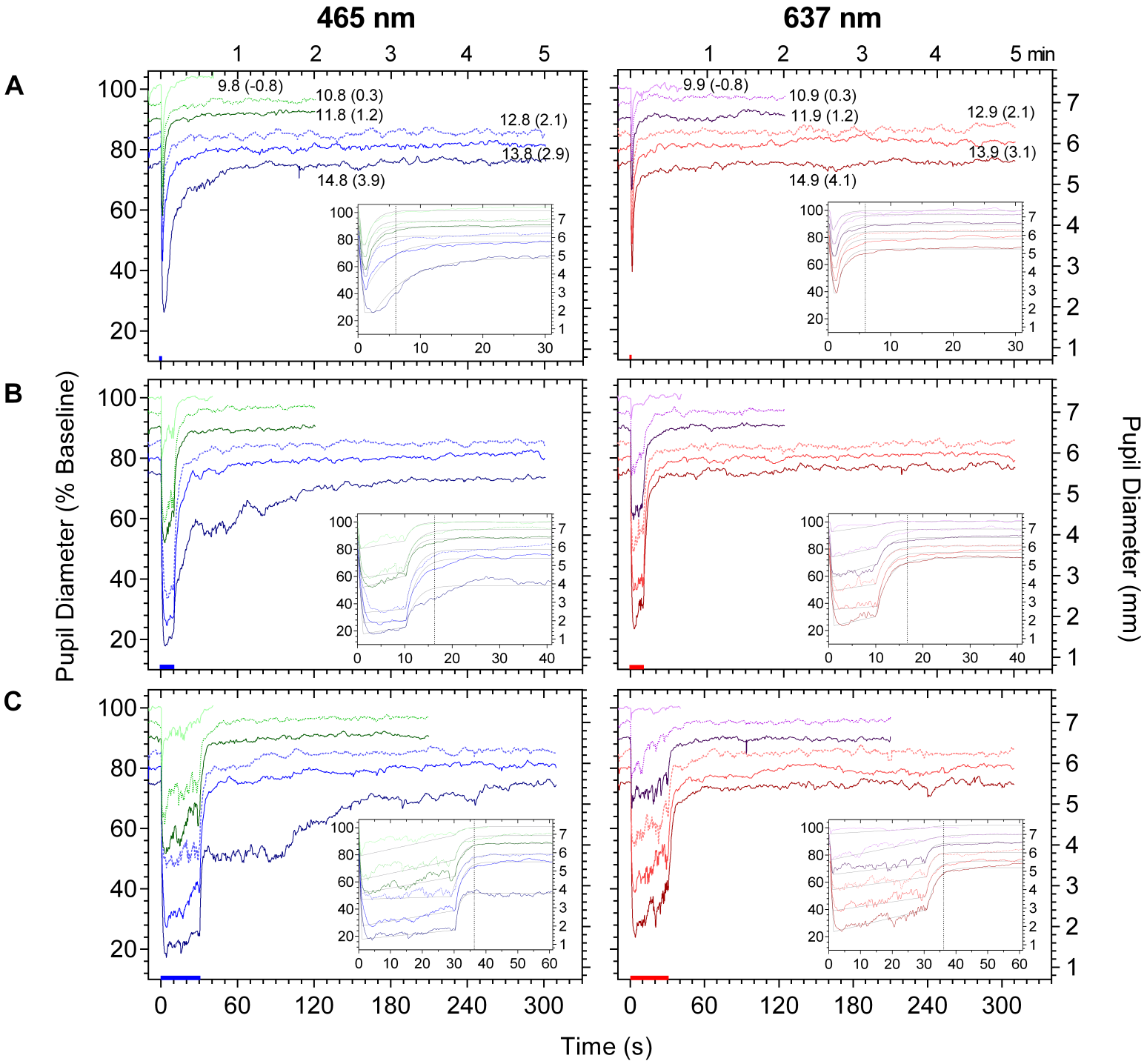
465 nm
637 nm
A
B
C
1
2
3
4
5
5 min
9.8 (-0.8)
10.8 (0.3)
11.8 (1.2)
12.8 (2.1)
13.8 (2.9)
14.8 (3.9)
9.9 (-0.8)
10.9 (0.3)
11.9 (1.2)
12.9 (2.1)
13.9 (3.1)
14.9 (4.1)
Pupil Diameter (% Baseline)
Pupil Diameter (mm)
Time (s)
0
60
120
180
240
300

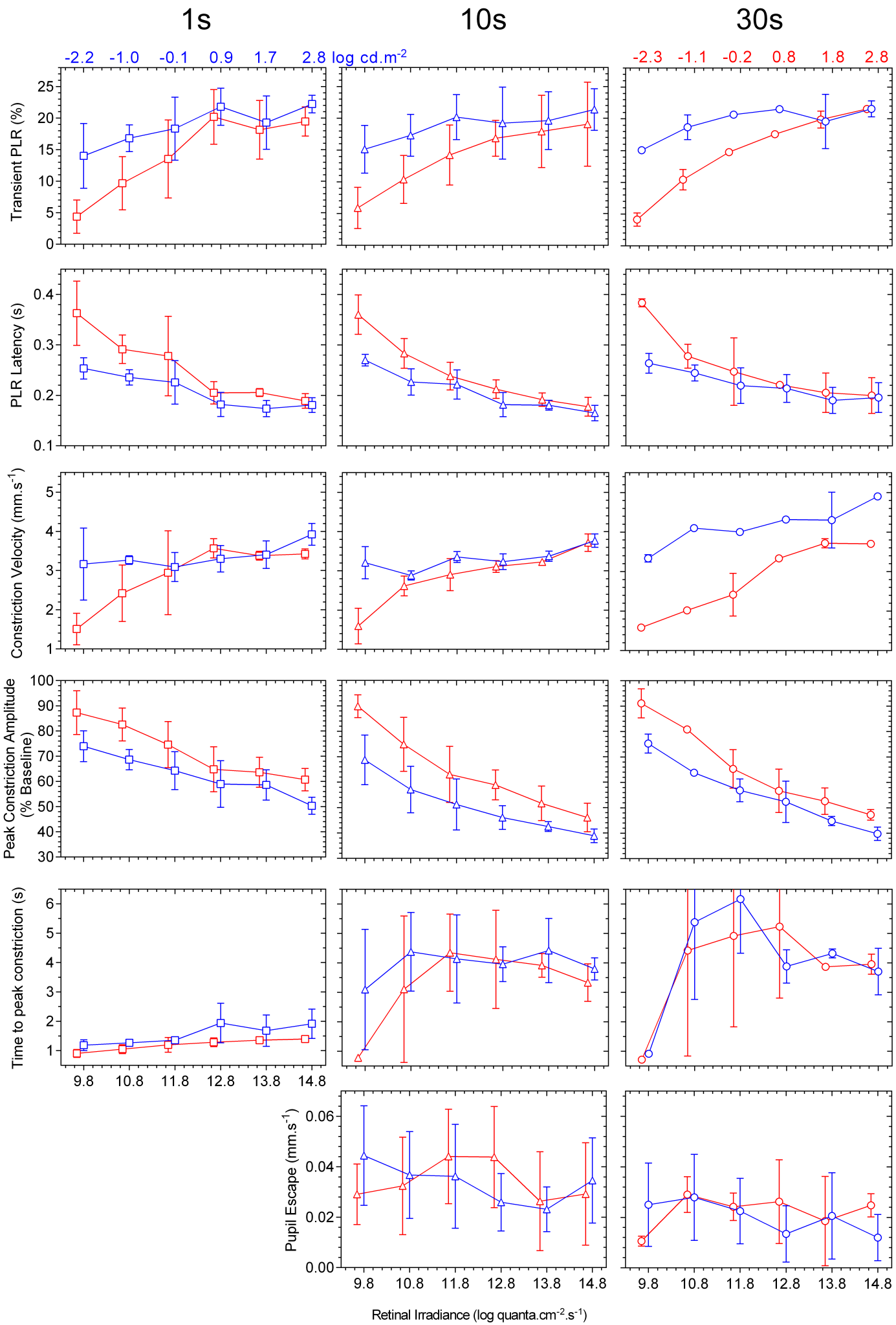
1s
10s
30s
-2.2 -1.0 -0.1 0.9 1.7 2.8 log cd.m-2
-2.3 -1.1 -0.2 0.8 1.8 2.8
Transient PLR (%)
PLR Latency (s)
Constriction Velocity (mm.s-1)
Peak Constriction Amplitude (% Baseline)
Time to peak constriction (s)
Pupil Escape (mm.s-1)
Retinal Irradiance (log quanta.cm-2.s-1)

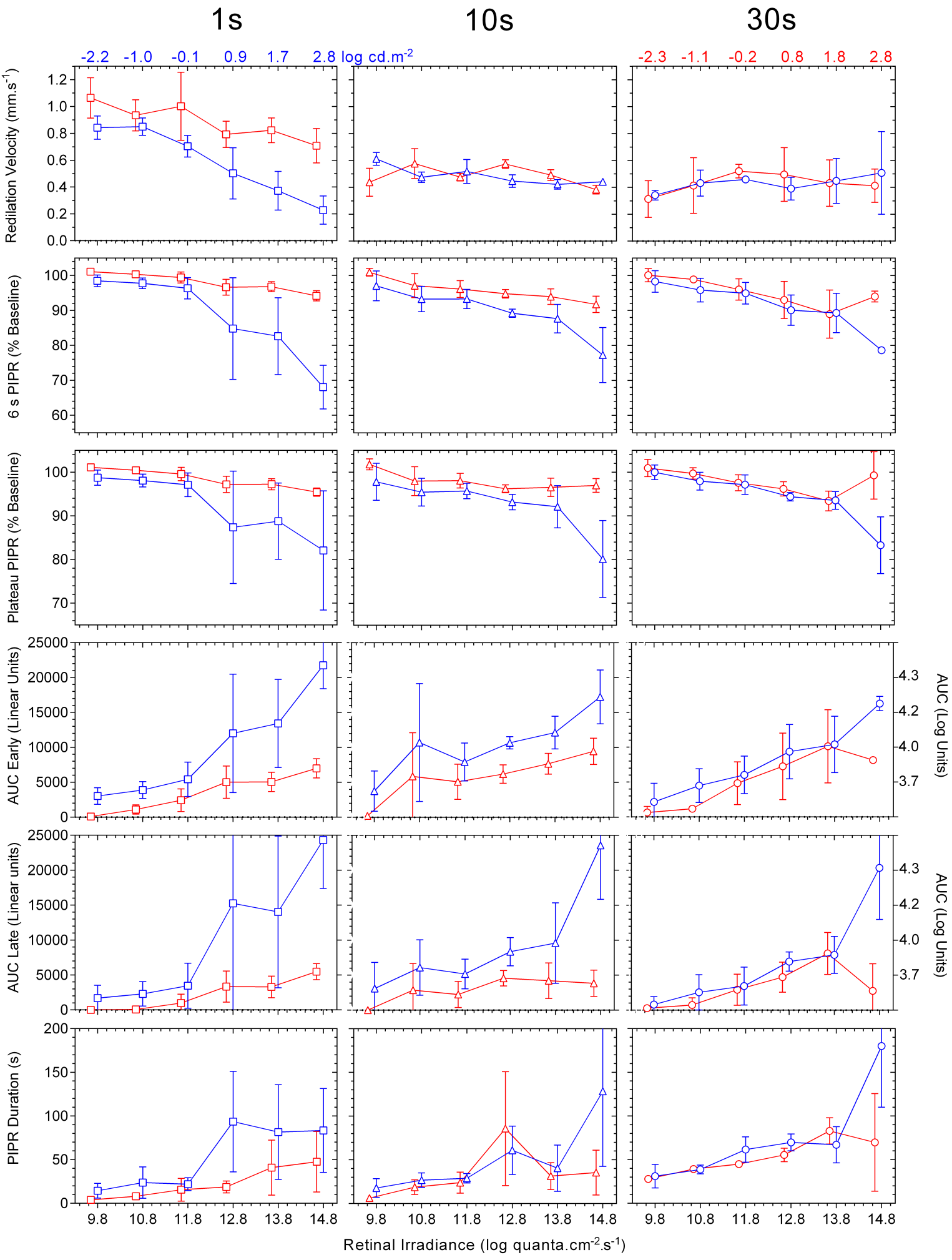
1s
10s
30s
-2.2 -1.0 -0.1 0.9 1.7 2.8 log cd.m-2
-2.3 -1.1 -0.2 0.8 1.8 2.8
Redilation Velocity (mm.s-1)
6 s PIPR (% Baseline)
Plateau PIPR (% Baseline)
AUC Early (Linear Units)
AUC Late (Linear units)
AUC (Log Units)
PIPR Duration (s)
Retinal Irradiance (log quanta.cm-2.s-1)

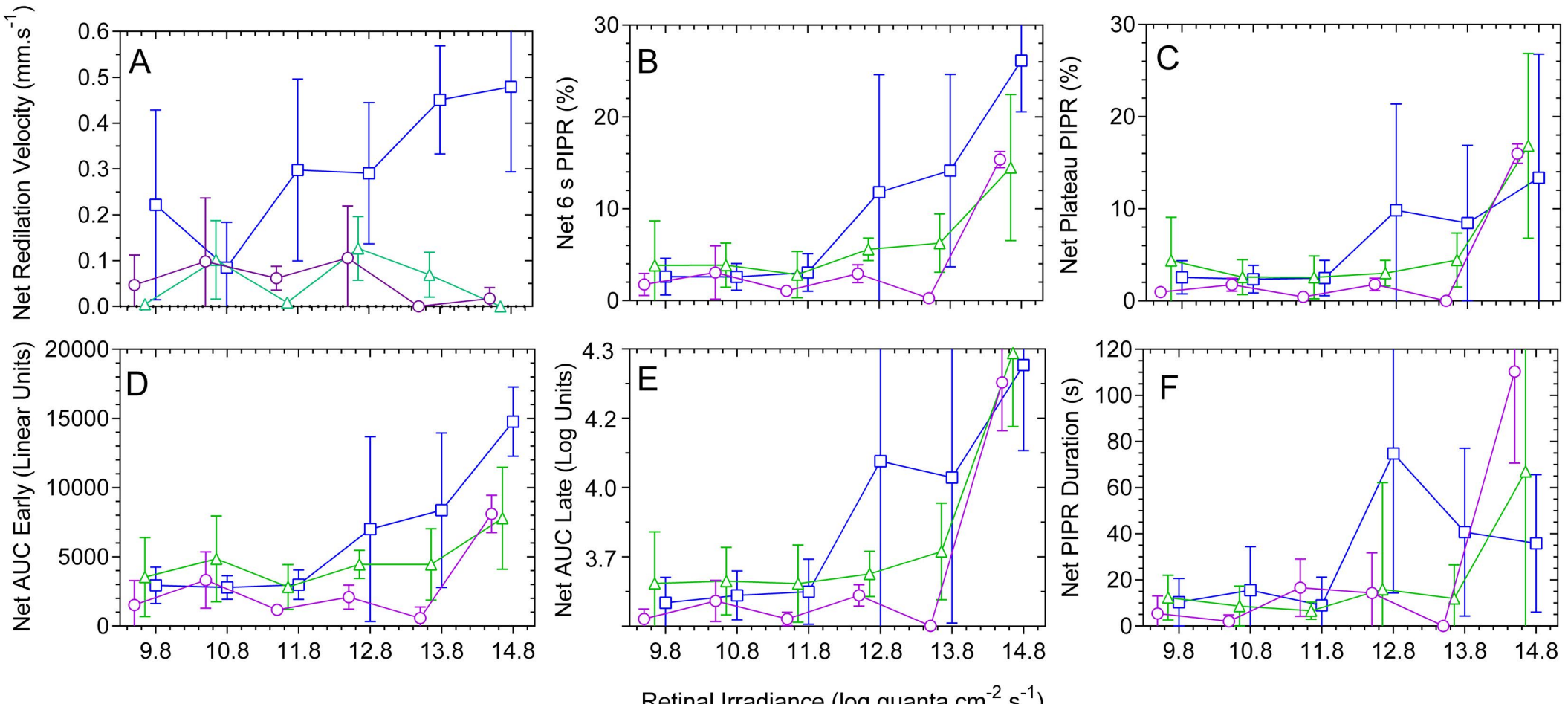
A
B
C
D
E
F
Net Redilation Velocity (mm.s-1)
Net 6 s PIPR (%)
Net Plateau PIPR (%)
Net AUC Early (Linear Units)
Net AUC Late (Log Units)
Net PIPR Duration (s)
Retinal Irradiance (log quanta.cm-2.s-1)
0.0
0.1
0.2
0.3
0.4
0.5
0.6
0
10
20
30
0
5000
10000
15000
20000
3.7
4.0
4.2
4.3
0
20
40
60
80
100
120
9.8
10.8
11.8
12.8
13.8
14.8

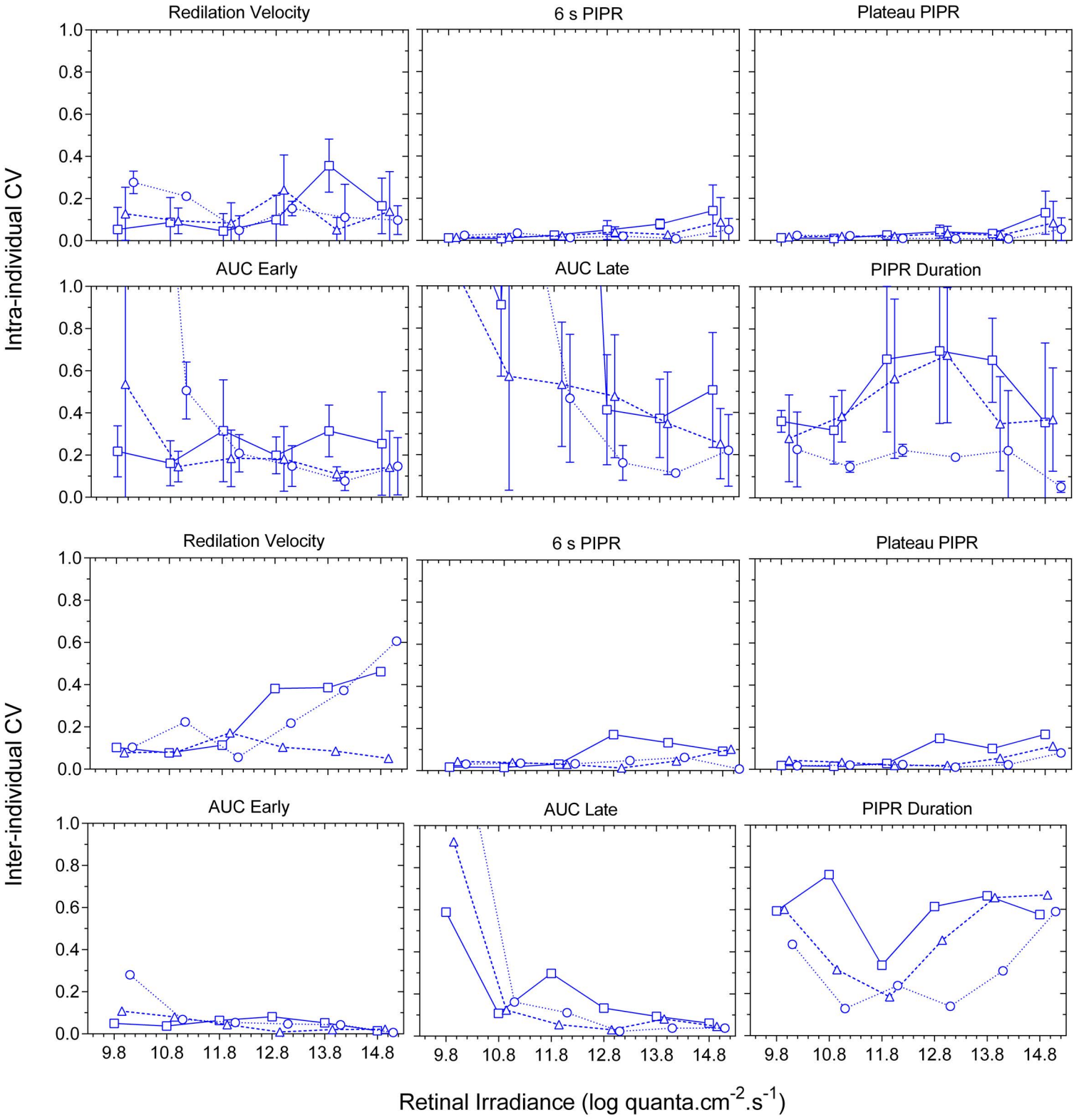
Redilation Velocity
6 s PIPR
Plateau PIPR
AUC Early
AUC Late
PIPR Duration
Intra-individual CV
Redilation Velocity
6 s PIPR
Plateau PIPR
AUC Early
AUC Late
PIPR Duration
Inter-individual CV
0.0
0.2
0.4
0.6
0.8
1.0
9.8
10.8
11.8
12.8
13.8
14.8
Retinal Irradiance (log quanta.cm-2.s-1)